Measurements of Intracranial Pressure and Compliance Index Using 1.5-T Clinical MRI Machine

Hideki ATSUMI[*1], Mitsunori MATSUMAE[*1], Akihiro HIRAYAMA[*1] and Kagayaki KURODA[*2]

[*1]*Department of Neurosurgery, Tokai University School of Medicine*
[*2]*Course of Information Science and Engineering, Tokai University Graduate School of Engineering*

Objective: To assess a newly proposed noninvasive technique for evaluating intracranial pressure (ICP) index and brain compliance (BC) index based on an inverse analysis of a brain-circulation-equivalent electrical circuit (EC) model, in which cerebrospinal fluid (CSF) flow and arterial flow rates measured by using the phase contrast method are used as currents.
Materials and Methods: Quantitative phase contrast flow measurements were performed by using a 1.5-T scanner for 25 volunteers and 23 patients with chronic increased ICP state. Bilateral carotid and verrtebral arteries and CSF flows were modeled by a pair of electrical circuits inductively coupled by a transformer. The ICP index was defined as the voltage of the second order circuit, while the BC index was calculated as the ratio between the mutual indeuctance of the transformer and the reactance in the second order circuit.
Results: The ICP index obtained by the EC correlated well with the pressure gradient obtained by the Navier-Stokes Technique (NS-PG). The combination of NS-PG and BC index by the EC appeared to be appropriate for characterizing the brain circulation status of the volunteers.
Conclusion: This noninvasive ICP and BC index measurement technique is more useful for asessment of intracranial condition.

Key words: noninvasice measurement, phase contrast method, intracranial pressure index, brain compliance index

INTRODUCTION

Intracranial pressure (ICP) is measured for monitoring in severe clinical central nervous system conditions such as head injury and cerebrovascular disease. In such neurological monitoring, ICP measurements are performed at the bedside in the intensive care unit, and real-time monitoring would be ideal for this purpose. Currently, routine ICP monitoring uses a pressure transducer introduced into the cerebral ventricle, cerebral parenchyma, and subdural space. Indeed this type of monitoring technique is invasive, but simultaneous bedside monitoring is needed and unavoidable to improve outcome of critical care. Some patients exhibit gradual increases in ICP, e.g., as a result of progressive tumor growth, meningitis, and pseudotumor cerebri. These patients' ICP increase becomes chronic. Such chronic increase is also recognized in patients with hydrocephalus, in which enlargement of the ventricular system occurs. Measurement of ICP is important for the diagnosis and management of chronic conditions. For such patients, there is considerable interest in finding a noninvasive way to estimate ICP. To clarify the cause of chronic increase in ICP, not only morphological assessment but also estimation of ICP itself is very helpful.

Recently, various technologies have been designed to determine ICP noninvasively. Schmidt *et al.* measured arterial flow velocity in the middle cerebral artery using ultrasound to predict relative increases in ICP wave forms noninvasively [1]. Schoser *et al.* demonstrated a linear relationship between mean ICP and maximum venous blood flow velocity in the deep vein structures [2]. Shakhnovich *et al.* [3] and Ueno *et al.* [4] estimated ICP by ultrasound as well. In 2000, Alperin *et al.* first developed an MRI method of measuring ICP as well as a brain compliance (BC) indexes [5]. They estimated pressure gradient (PG) rather than ICP using phase-contrast (PC) magnetic resonance (MR) imaging of the cerebrospinal fluid (CSF) flow and the Navier-Stokes' equation. After they demonstrated that PG correlate well with ICP, which was measured by an invasive pressure probe, they derived BC index by using the monoexponential relationship between PG and intracranial compartment volume change over a cardiac cycle obtained also by the PC-based arterial and venous blood flow quantification. As an alternative approach, we have proposed a noninvasive technique to evaluate ICP index and brain compliance (BC) index based on an inverse analysis of a brain-circulation-equivalent electrical circuit model, in which MR-measured CSF flow and blood flow rates are used as electrical currents [5]. Although the validity of the technique was assessed by phantom experiments followed by volunteer experiments, the relationships of the ICP and BC indexes with corresponding results ob-

Mitsunori MATSUMAE, Department of Neurosurgery, Tokai University School of Medicine, 143 Shimokasuya, Isehara, Kanagawa 259-1193, Japan
Tel: +81-463-93-1121 FAX: +81-463-94-9894 E-mail: mike@is.icc.u-tokai.ac.jp

tained by the Navier-Stokes-based approach remained unclear.

Thus in the present work, the equivalent circuit technique and the Navier-Stokes' equation technique will be directly compared and complementary use of these techniques will be examined. All the human studies were approved by the internal review board of our institution and appropriate informed consent was obtained from the volunteers.

METHODS

Image acqsition

Quantitative phase contrast flow measurements were performed in 25 healthy volunteers (23–63 years of age) and 23 patients (8–78 years of age) with chronic increase in ICP due to brain tumors using a 1.5-T scanner (Gyroscan, Philips; Best, The Netherlands) with the following settings: TR/TE/FA, 20.1 ms/12.7 ms/10 degrees; slice thickness, 10 mm; FOV, 160 × 160 mm^2; spatial matrix, 256 × 256; VENC, 80–100 cm/s for blood, and 5–10 cm/s for CSF. Scanning was performed with a single oblique slice placed to be perpendicular to the celebrospinal space at the level of the foramen magnum of each volunteer. Data were acquired continuously with peripheral monitoring of cardiac pulse form, and then sorted retrospectively to reconstruct a set of velocity images at 16 cardiac phases.

In addition to the above mentioned experiments with the volunteers normally ventilating, another experiments on six volunteers (21–25 years of age, male) with hyper-ventilating condition were examined, in order to observe changes of the indexes. During similar flow acquisitions described above, each volunteer was first requested to relax but to keep awake. Before this observation, the volunteers sit at least for 30 minuits in the MRI stuite to have good rest. In the following observation, the patients were requested to have deep and continuous breathing (15–20 times/min) to be slightly hyperventilated. The volunteers then relaxed and kept awake again during scanning. The acquisition settings were identical with the above.

To examine the effect of pre-experimental conditions of the volunteers, each patient was also requested to have walking exercise (going up and down stairs with around 400 steps) immediately before scanning in the separate experiments.

Image processing

The voxels with arterial, venous and CSF flows were differentiated to each other and segmented from the surrounding stationary tissues by using a pulsatility-based segmentation (PUBS) technique [6]. The reference points for PUBS processing were manually set and the segmentation result was visually assessed by skilled neurosurgents (MM or AH). The velocities of the flows at each voxel were then multiplied with the cross sectional area of a voxel (0.875 × 0.875 mm^2) to calculate the flow volume per an unit time. Then the time seriese of the total flow rates at the carotid and vertebral arteries, the internal jugular veins, and the CSF space were obtained.

Equivalent circuit technique

To understand the physiological parameter such as pressure gradient of the CSF is very useful to determind the cause CSF abnormal distribution in the skull. To calculate a pressure gradient of CSF from the data of MRI, we have to rearrange several factors such as arterial pulsation, venous circulation, brain pulsation into simple electrical circuit model. To make the simple electrical circuit model is necessary to clarify the value of pressure gradient. The equivalent circuit technique, with two major brain circulation systems including blood and CSF flows, was modeled by the electrical circuit shown in Fig. 1. Relationships between the circuit components of the fluid and the electrical systems are shown in Table. The brain circulation was analyzed by inversely determining the circuit elements at the second side circuit (X_2, R_2, M) based on the currents given by the arterial blood flow rate (I_1) and the CSF flow rate (I_3). In this inverse analysis, the above mentioned flow rates were used after Fourier transformation from time domain to frequency domain in order to perform the circuit analysis by so called complex calculation technique known in electrical engineering. The estimation function of the inverse analysis was the sum of the square error of the estimated CSF flow rate from the measured one. The parameters, X_2, R_2 and M were estimated by the simplex method. One thousand sets of the initial conditions were given to the parameters, and the estimated values were mapped in the X_2-R_2-M space.

Brain circulation was analyzed inversely by determining the circuit elements at the second-order side of the circuit (X_2, R_2, M) based on the currents obtained as the arterial blood flow rate (I_1) and CSF flow rate (I_2). The BC index (BCI) was defined as M/X_2, while the ICP index (ICPI) was defined as the voltage ($V_2 = (R_2 + jX_2)I_2 \approx jX_2 \cdot I_2$ ($R_2 << X_2$)) of the circuit.

Navier-Stokes' equation technique

In the Navier-Stokes technique, the same data sets were used for calculating the pressure gradient in the CSF flow appearing in the following equation;

$$\nabla p = -\rho \frac{\partial v}{\partial t} - \rho(v \cdot \nabla)v + \mu \nabla^2 v \ [1]$$

where p is pressure, v is CSF flow velocity, ρ is density and μ is viscosity. Because of the low viscosity and non-convective properties of the CSF flow, the second and third term of the right side of the equation could be neglected. Correlation between the resultant pressure gradient obtained by this equation and ICP index obtained by the equivalent circuit technique was evaluated.

RESULTS

Fig. 2 shows the relationship between the peak-to-peak CSF (CSF_{pp}) and the peak-to-peak intracranial pressure index obtained as the second-order side voltage (V2) in the equivalent circuit model ($EC\text{-}ICPI_{pp}$). Fig. 3 shows the relationship between the peak-to-peak CSF flow and the peak-to-peak pressure gradient obtained by the Navier-Stokes equation ($NS\text{-}PG_{pp}$). Fig. 4 shows relationships between peak-to-peak intracranial

a

b
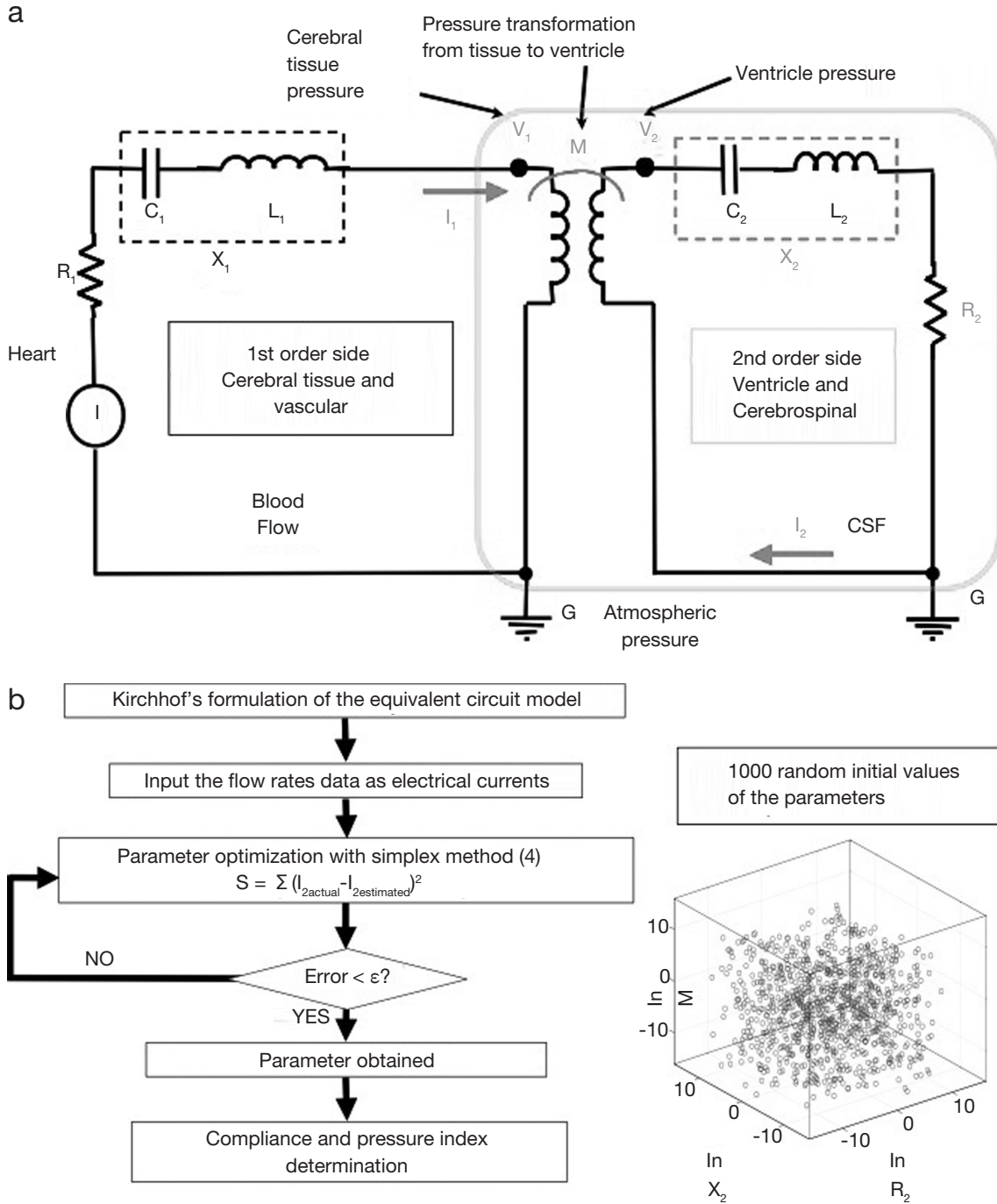
Fig. 1 a : The equivalent circuit technique, with two major brain circulation systems including blood and CSF flows, was modeled by the electrical circuit.
b : The algorithm of inverse analysis for determination of compliance and pressure index.

pressure index (EC-ICPI$_{pp}$) and the pressure gradient (NS-PG$_{pp}$). Fig. 5 shows relationships between the ratio of peak-to-peak CSF (CSF$_{pp}$) and arterial blood (Art$_{pp}$) flows and the brain compliance index defined as the ratio of the mutual inductance (M) over the reactance (X$_2$) in the equivalent circuit model (EC-BCI).

The ICP index obtained by the equivalent circuit technique (EC-ICPI) correlated well with the pressure gradient obtained by the Navier-Stokes Technique (NS-PG) for both healthy and patient volunteers. The NS-PG was more directly calculated with CSF flow data. For the BC index, venous flow must be used in

NS-PG to calculate the total fluid volume change. In the equivalent circuit technique, venous flow was not required since the BC index (EC-BCI) was calculated as the ratio between the mutual inductance (M) and the reactance (X$_2$). EC-BCI correlated with the ratio of the CSF flow and the blood flow. Based on these findings, the combination of NS-PG and EC-BCI appeared to be appropriate for characterizing the brain circulation status of the volunteers. Fig. 6 shows sequential changes of EC-BCI in a healthy volunteer, while Fig. 7 shows age-related change in EC-ICPI$_{pp}$. Fig. 8 shows age-related change in NS-PG$_{pp}$. BCI tended to decrease

c

Phantom with current/voltage mea't
→ converge to a value

$S=(S(V_{2actual}-V_{2estimated})^2)^{1/2}$

→The algorithm was validated

Volunteer with current mea't only
→ converged to a certain ratio

$S=(S(I_{2actual}-I_{2estimated})^2)^{1/2}$

→The ratio of the parameters uniquely obtained
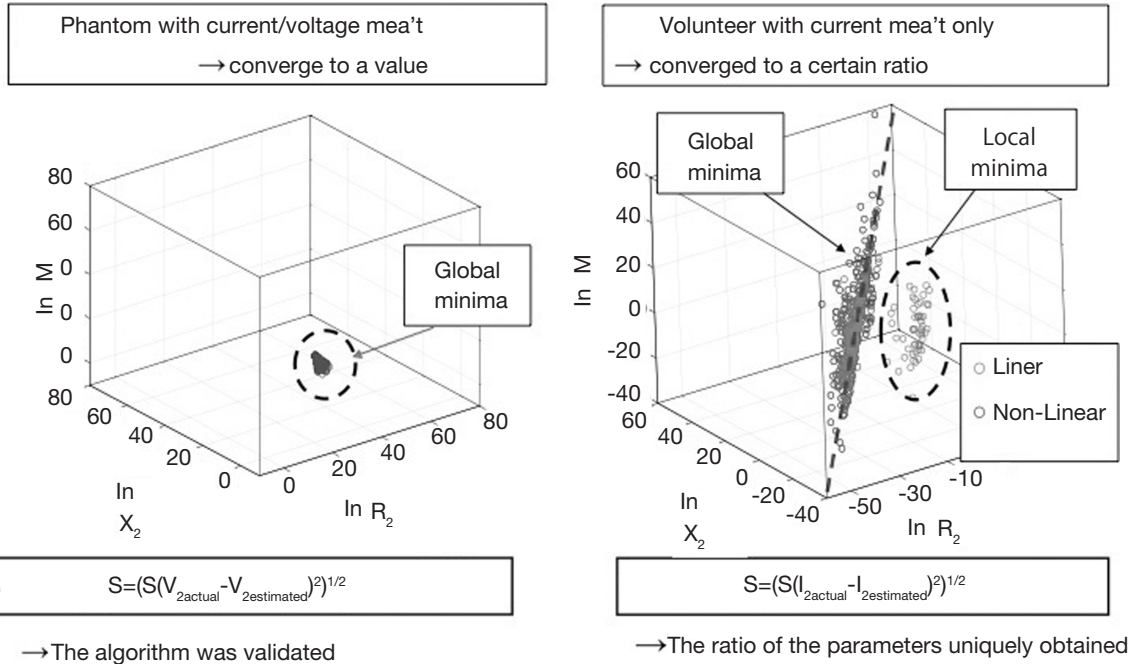
d
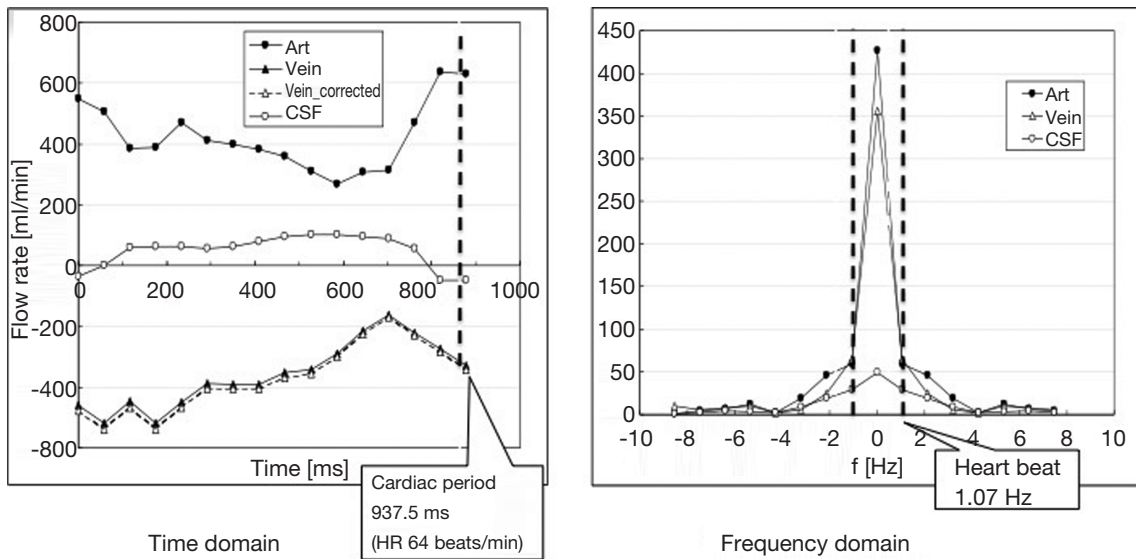
Fig. 1 (Continue)
    c : The solutions of inverse analysis for validation of the algorithm.
    d : Two types analysis (time domain and frequency domain) of flow rate in a human volunteers.

with age. Moreover, EC-ICPI$_{pp}$ and NS-PG$_{pp}$ were negatively correlated with age. For comparison between physiological and non-physiological conditions, hyperventilation was performed by the healthy volunteers. Five of the 6 volunteers exhibited dramatic decrease in BCI after the hyperventilation task (Fig. 9). Three volunteers exhibited decrease in BCI without any changes in ICPI (Fig. 9), and 2 volunteers exhibited decreases in both BCI and ICPI. One volunteer exhibited increased BCI without changes in ICPI (Fig. 9). Compared with the healthy volunteers, the patient group tended to exhibit slight increases in ICPI and

decreases in BCI. However, most of the patients and healthy volunteers had overlapping values. In particular, 3 patients who had exceeded pressure index above 0.015, exhibited dramatic increases in ICPI with decrease in BCI. These patients complained headache, nausea, and some difficulty of patient's daily life at the time of MRI study. Patients MRI showed that massive volume of brain tumor in the intracranial parenchyma with severe perifocal edema. Clinically and morphologically those patients classify into a chronic increased ICP condition.

Table Relationships between the circuit components of the fluid (left side) and the electrical systems (right side).

Fluid	Electrical
Blood circulation	1st order circuit
CSF circulation	2nd order circuit
Ventricle wall	Transformer
Heart	Current source
Arterial flow rate	Current I_1
Venous flow rate	$I_2 (= I_1)$
CSF flow rate	I_3
Atmospheric pressure	Ground voltage, G
Pressure on the brain tissue side	Voltage, V_1
Pressure on the ventricle side	V_2
Compliance and intertance	Reactance
for the blood circulation	X_1
for the CSF circulation	X_2
Resistance	Resistance
for the blood circulation	R_1
for the CSF circulation	R_2
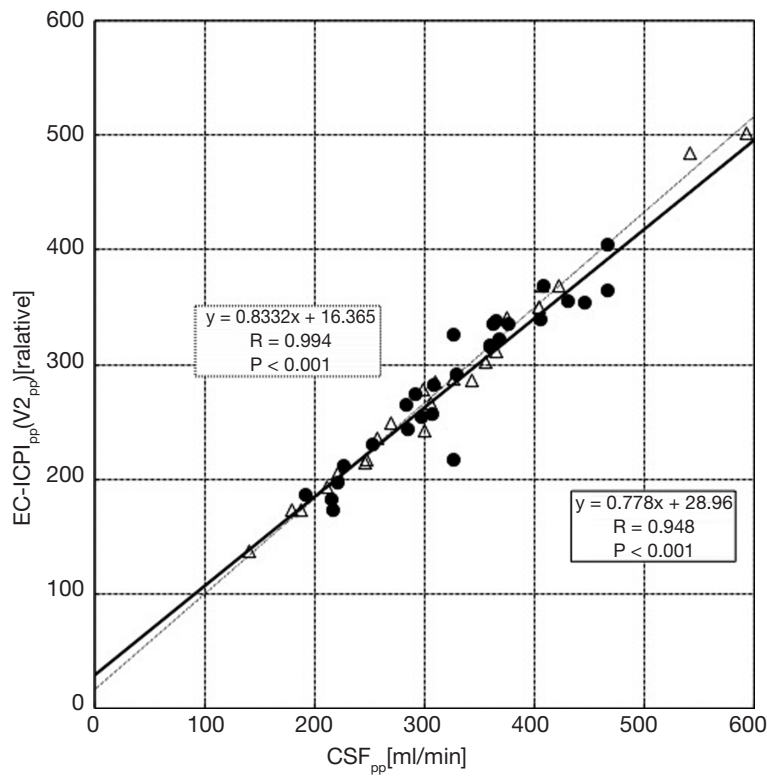
Fig. 2 Relationships between the peak-to-peak CSF flow (CSF_{pp}) and the peak-to-peak of the intracranial pressure index obtained as the second-order side voltage (V_2) in the equivalent circuit model ($EC\text{-}ICPI_{pp}$). Triangle and dot line indicates patients data. Black dot and continuous line indicates healthy volunteer's data.
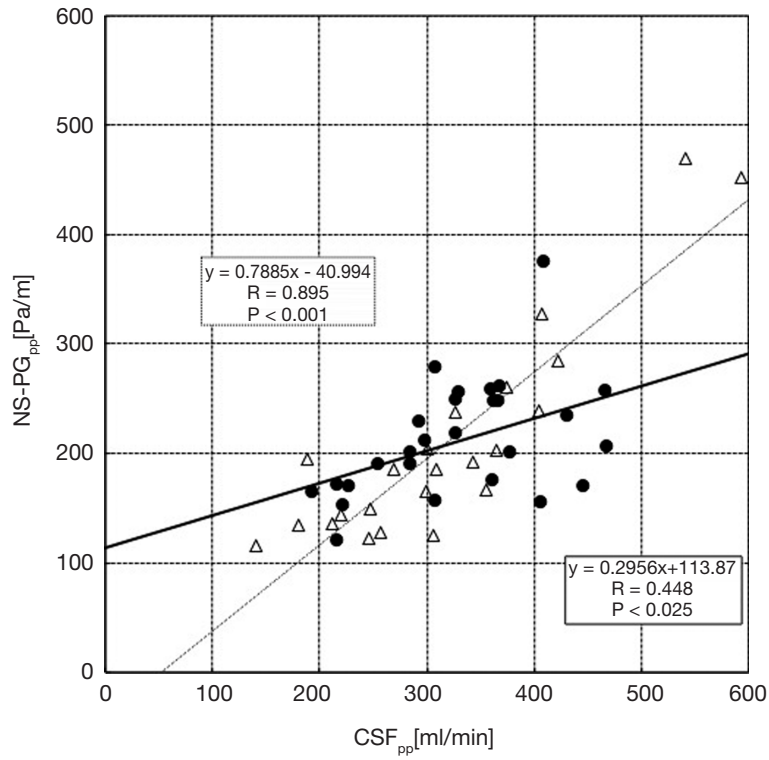
Fig. 3 Relationships between the peak-to-peak CSF flow (CSF$_{pp}$) and the peak-to-peak pressure gradient obtained by the Navier-Stokes equation (NS-PG$_{pp}$). Black dot and continuous line indicates healthy volunteer's data.
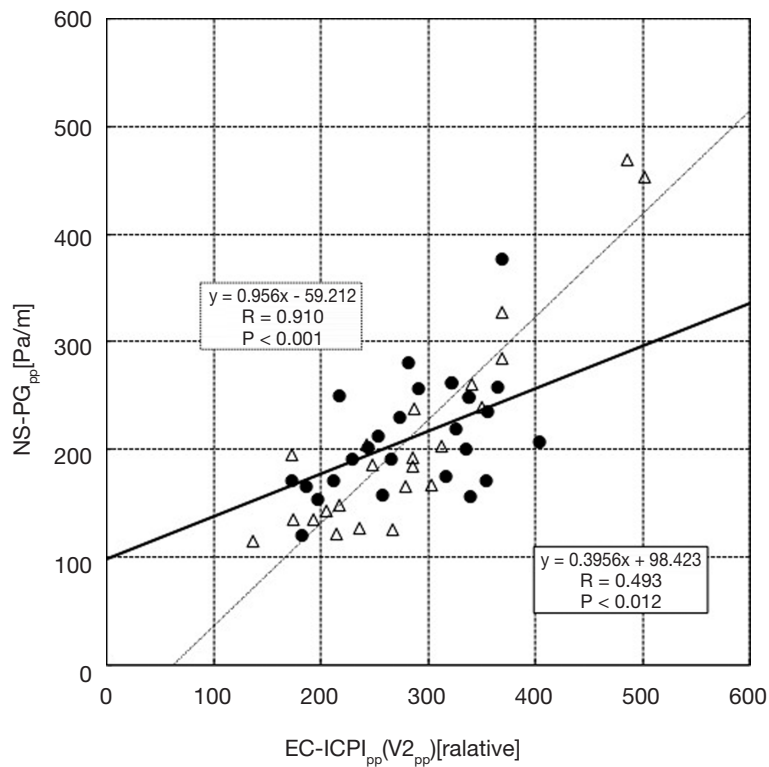
Fig. 4 Relationships between the peak-to-peak of the intracranial pressure index (EC-ICPI$_{pp}$) and the pressure gradient (NS-PG$_{pp}$). Black dot and continuous line indicates healthy volunteer's data.

$$y = 0.9873x + 0.0092$$
$$R = 0.948$$
$$P < 0.001$$

$$y = 0.9787x + 0.0023$$
$$R = 0.966$$
$$P < 0.001$$

EC-BCI (MIX2) [ralative]

CSF_{pp}/Art_{pp}[nondimensional]
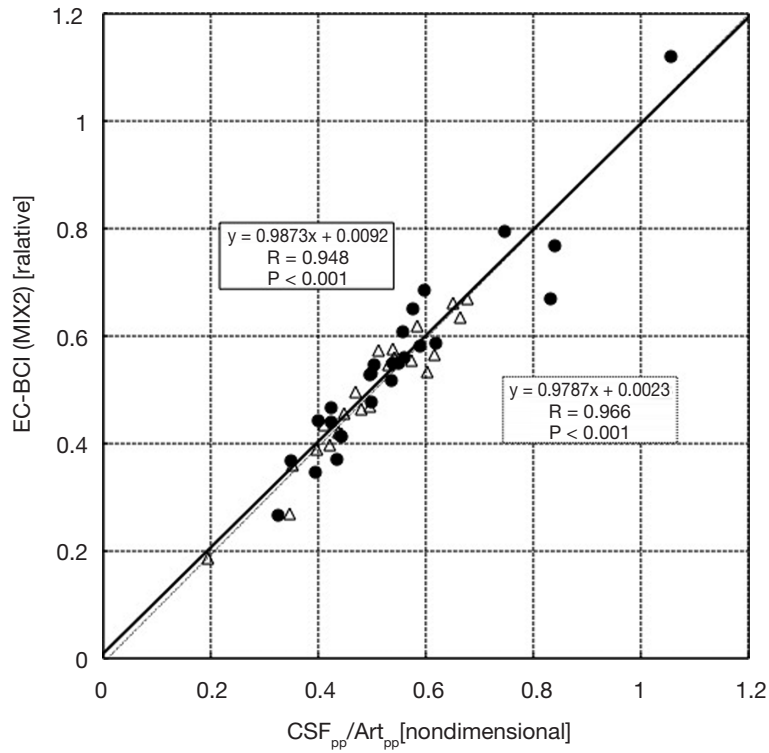
Fig. 5 Relationships between the ratio of peak-to-peak CSF (CSF_{pp}) and arterial blood (Art_{pp}) flows and the brain compliance index defined as the ratio of the mutual inductance (M) over the reactance (X_2) in the equivalent circuit model (EC-BCI). Black dot and continuous line indicates healthy volunteer's data.

$$y = -0.0028X + 0.6708$$
$$R = 0.210$$
$$P = 0.31$$

$$y = -0.0022X + 0.5997$$
$$R = 0.334$$
$$P = 0.12$$

BCI [relative]

Age[yo]
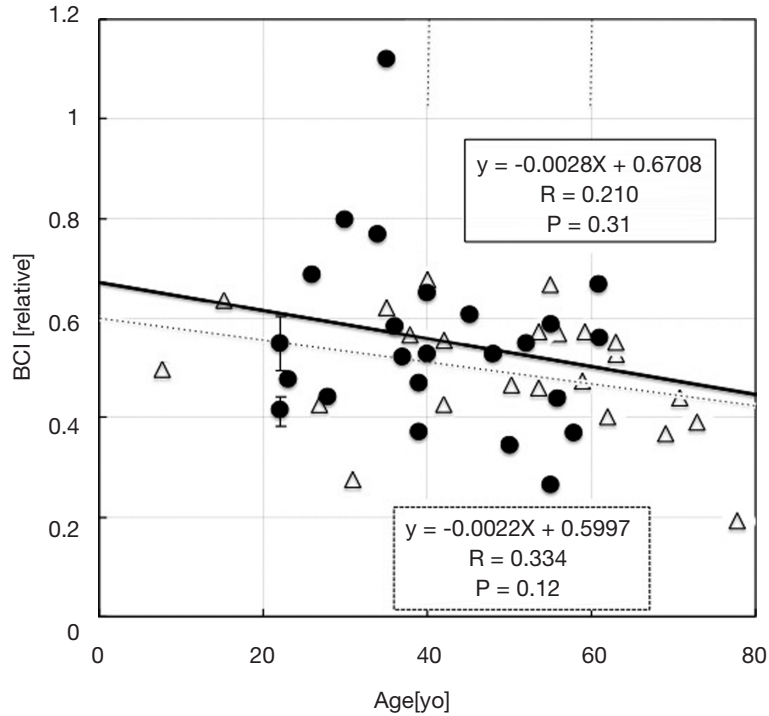
Fig. 6 Age-related change of the brain compliance index (EC-BCI). Black dot and continuous line indicates healthy volunteer's data.
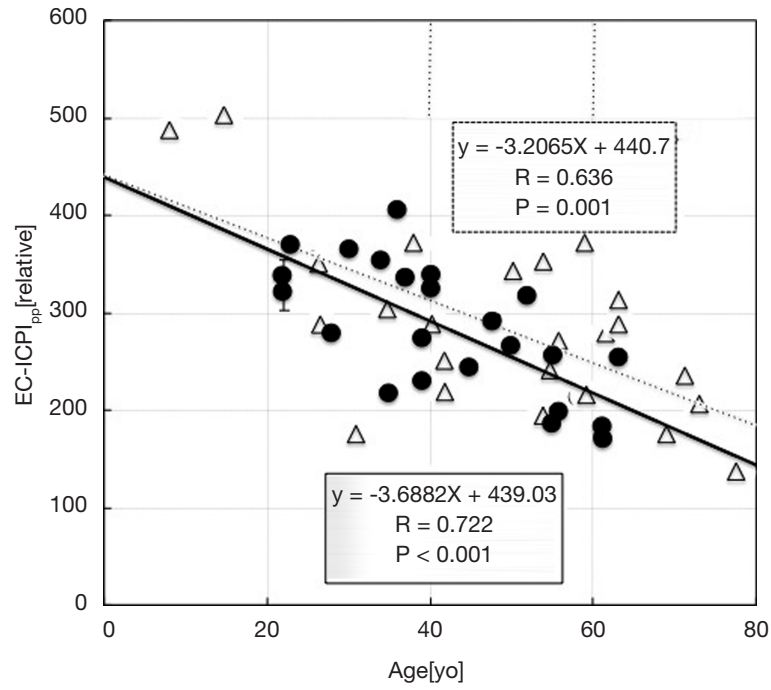
Fig. 7 Age-related change of the peak-to-peak of the intracranial pressure index (EC-ICPI$_{pp}$). Black dot and continuous line indicates healthy volunteer's data.
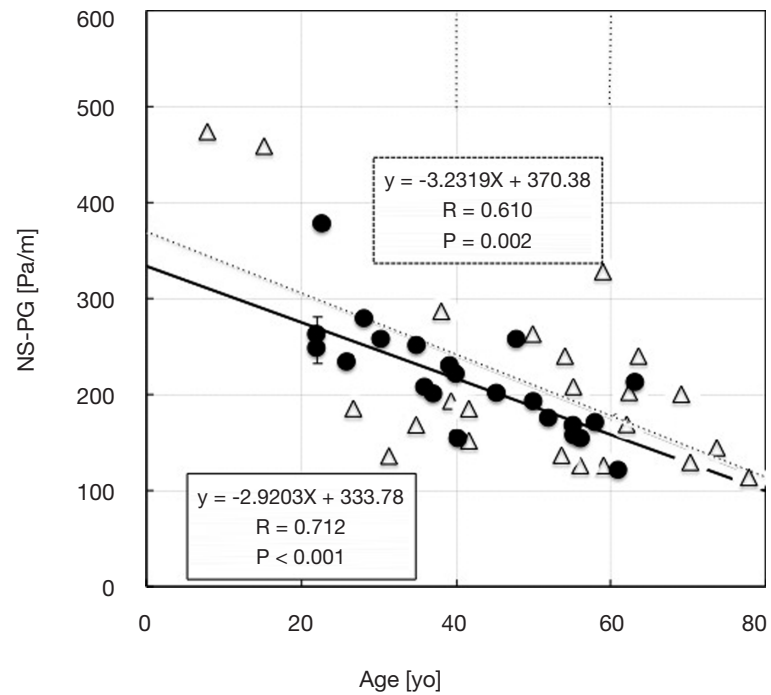
Fig. 8 Age-related change of the peak-to-peak of the pressure gradient (NS-PG$_{pp}$). Black dot and continuous line indicates healthy volunteer's data.
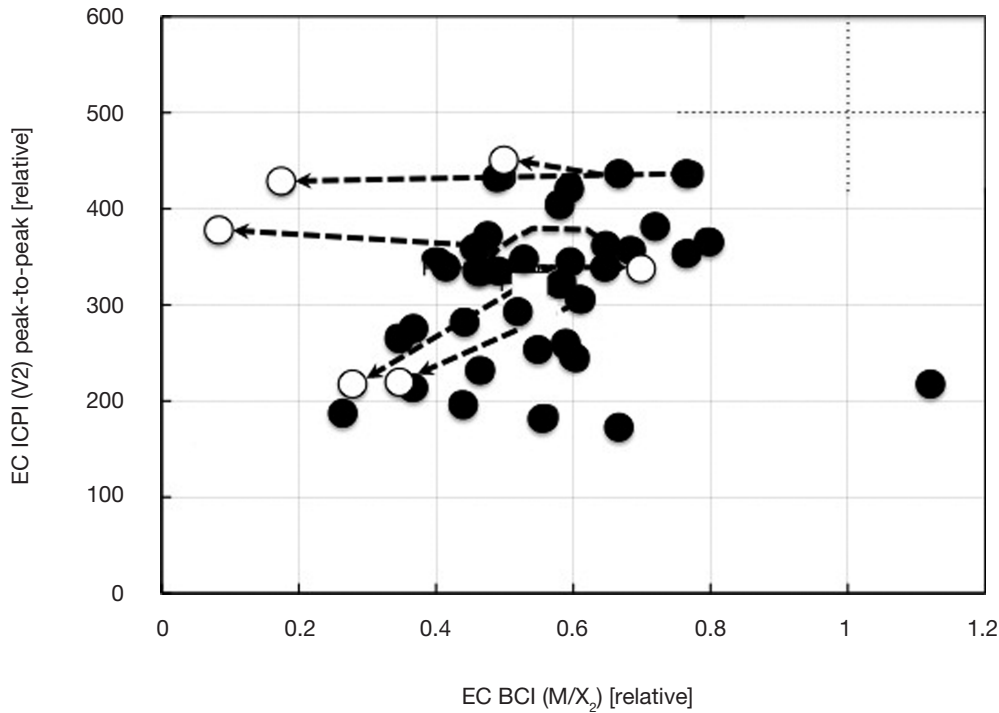
Fig. 9 Changes of the brain compliance and ICP index after the hyperventilation. The arrows indicate the changes of the indexes with hyperventilation. Black dot indicates healthy volunteer's data before hyperventilation task. White circle indicates healthy volunteer's data after hyperventilation.

DISCUSSION

The ICP index obtained by EC-ICPI correlated well with the pressure gradient obtained by NS-PG for both healthy volunteers and patients. NS-PG was more directly calculated with CSF flow data. For BC index, artery and venous flows must be used in NS-PG to calculate the total fluid volume change. In the equivalent circuit technique, the venous flow was not required, since EC-BCI was calculated as the ratio between the mutual inductance (M) and the reactance (X_2). EC-BCI correlated with the ratio of the CSF flow and the blood flow. Based on these findings, the combination of NS-PG and EC-BCI appeared to be appropriate for characterizing the brain circulation status of the volunteers. Using EC-ICPI and EC-BCI, we found some clinical differences between healthy volunteers and patients with chronically increased ICP. In particular, 6 of 9 patients had increased EC-ICPI with decreased EC-BCI. This result provides significant noninvasive physiological information. Four of 9 patients exhibited slightly decreased EC-BCI but overlapping EC-ICPI. We have excluded patients into MR scanner those who severely increased ICP in clinically. This is the reason why 4 of 9 patients overlapped their EC-ICPI and EC-BCI. This is a limitation of our study.

O'Connell emphasized the contribution of the cardiac and respiratory pulses in the CSF pressure to the mixing of cranial and spinal fluid [7]. Pulsatile movement in the ventricular system was particularly observed in the IIIrd ventricle, providing a pump action that consisted largely of a rhythmic squeezing in the IIIrd ventricle. In 1977, Ekstedt reported the relationship between CSF pressure and CSF flow in a human subject [8]. The results clearly demonstrated an approximately linear relationship. We could therefore estimate CSF pressure using CSF flow determined by MR. It is known that decrease in CO_2 tension in the blood induced by hyperventilation causes a moderate decrease in cerebral blood flow. The decrease in cerebral blood flow is explained by vasoconstriction of cerebral vessels. In the present study, the decrease in arterial flow in one cardiac cycle averaged from 17% to 40% during hyperventilation. All healthy volunteers except one in the present study exhibited decreases in BCI during hyperventilation, and after hyperventilation EC-BCI returned to within normal range. This may explain the vasoconstriction in brain parenchyma. Interestingly, 3 patients exhibited increased ICPI with dramatic decrease in EC-BCI. These 3 patients had huge meningiomas and obstructive hydrocephalus. These patients complained of headache and nausea with papilledema. Clinically, these 3 patients were classified as having moderately increased ICP. Therefore, the electrical equivalent circuit method may provide the useful information to assess the fine intracranial condition between physiological and pathological condition.

This noninvasive measurement of EC-ICPI and EC-BCI by MR enables understanding of the intracranial environment. Clinically, the role of MR-based ICP measurement may differ from that of the current invasive technique. Whereas invasive monitoring provides continuous ICP measurements usually obtained in the intensive care unit for patients with severe neurological disease, MR assessment of ICP is not continuous. There are several clinical advantages to use of this noninvasive ICP measurement technique by MRI in

understanding the intracranial environment, especially in patients with moderate neurological disease. Using the phase contast MR technique, we measure a detail of blood flow and CSF flow during one cardiac cycle. Based on these data, we estimate the intracranial pressure index and brain compliance index by electrical equivalent circuit method. We show that these index changes to response of intracranial condition with physiological and pathological condition. In order to assess the pathological condition using these indexes for clinical decision making, we will continue this research for understanding a normal rage of flows in the physiological condition not only one cardiac cycle but also respiration state. Moreover we apply this simple brain-circulation-equivalent electrical circuit model to understanding the velocity and pressure gradient of CSF in normal volunteer and patient [9].

GRANT INFORMATION

REFERENCES

1) Schmidt B, Klingelhöfer J, Schwarze JJ, Sander D, Wittich I. Noninvasive prediction of intracranial pressure curves using transcranial Doppler ultrasonography and blood pressure curves. Stroke. 1997; 28: 2465–2472.
2) Schoser BGH, Riemenschneider N, Hansen HC. The impact of raised intracranial pressure on cerebral venous hemodynamics: A prospective venous transcranial Doppler ultrasonography study. J Neurosurg. 1999; 91: 744–749.
3) Shakhnovich AR, Shakhnovich VA, Galushkina AA. Noninvasive assessment of the elastance and reserve capacity of the craniovertebral contents via flow velocity measurements in the straight sinus by TCD during body tilting test. J Neuroimaging. 1999; 9:141–149.
4) Ueno T, Ballard RE, Shuer LM, Cantrell JH, Yost WT, Hargens AR. Noninvasive Measurement of Pulsatile Intracranial Pressure Using Ultrasound. Acta Neurochirurgica, Supplement. 1998; 71: 66–69.
5) Alperin NJ, Lee SH, Loth F, Raksin PB, Lichtor T. MR-intracranial pressure (ICP): A method to measure intracranial elastance and pressure noninvasively by means of MR imaging: Baboon and human study. Radiology. 2000; 217: 877–885.
6) Alperin. NJ, Lee SH. PUBS: pulsatility-based segmentation of lumens conducting non-steady flow. Magn Reson Med. 2003; 49: 934–944.
7) O'Connell JEA: The vascular factor in intracranial pressure and the maintenance of the cerebrospinal fluid circulation. Brain. 1943; 66: 204–228.
8) Ekstedt J. CSF hydrodynamic studies in man. 1. Method of constant pressure CSF infusion. Journal of Neurology Neurosurgery and Psychiatry. 1977; 40: 105–119
9) Matsumae M, Hirayama A, Atsumi H, Yatsushiro S, Kuroda K. Velocity and pressure gradients of cerebrospinal fluid assessed with magnetic resonance imaging. J Neurosurg. 2014; 120: 218–227.